Arch. Metall. Mater. **65** (2020), 2, 555-563

DOI: 10.24425/amm.2020.132793

KUO-TSUNG HUANG[1], SHIH-HSIEN CHANG[2*], CHAN-YU CHUANG[2]

MICROSTRUCTURE AND PROPERTIES OF COMPOSITE PRODUCED BY VACUUM SINTERING OF VANADIS 4 EXTRA STEEL POWDER WITH TANTALUM CARBIDES AND FOLLOWING HEAT TREATMENT

In this study, different amounts of tantalum carbide (TaC) powders (5, 10 and 15 wt.%) are added to Vanadis 4 Extra steel powders. The composite powders are sintered at 1260, 1280, 1300, 1320, 1340 and 1360°C for 1 h, respectively. The experimental results showed that good mechanical properties (hardness 79.7 HRA, TRS 2246 MPa) were obtained by the addition of 10% TaC sintered at 1320°C for 1 h. Furthermore, the optimal sintered V4ES/TaC (Vanadis 4 Extra steel / TaC) composites after sub-zero treatment possess the highest hardness (80.9 HRA) and transverse rupture strength (TRS) values (2445 MPa), as well as a better polarization resistance (658.99 $\Omega \cdot cm^2$). After sub-zero treatment, the VC carbides decompose and re-precipitate refined VC carbides within the grains (VC carbides are formed in steel powder); moreover, the TaC particles are still uniformly distributed around the grain boundaries, which results in dispersion strengthening and precipitation hardening. The results clearly reveal that sub-zero heat treatment effectively improves the microstructure and strengthens the V4ES/TaC composite.

Keywords: Tantalum carbide, Vanadis 4 Extra steel, transverse rupture strength, polarization resistance, sub-zero heat treatment

1. Introduction

Vanadis 4 Extra steels are the powder metallurgical (P/M) cold work tool steels offering an extremely good combination of wear resistance and ductility. This makes it possible for consistent tool performance such as blanking and forming of austenitic stainless steel [1]. Powder metallurgy (P/M) is a process for forming near-net parts by heating compacted metal powders to just below their melting points [1,2]. Besides, P/M is thought to be the most common production technique for ceramic particles reinforced composites [3]. One of the advantages of P/M compared to other methods is having better control on the microstructure, where better distribution of the reinforcements is possible in P/M compacts [4].

Metal matrix composites (MMCs) possess significantly improved properties compared to unreinforced alloys. MMCs are new materials with different types of ceramics as reinforcement phase dispersed in the metal matrix. Additions of carbides such as, TaC, Cr_3C_2, or VC etc. to the powder mixtures are often done in order to increase the wear resistance for high-speed machining steel. These carbides are known to inhibit grain growth in high temperature of P/M process [5,6]. TaC is an extremely hard (Mohs hardness 9-10) refractory ceramic material. It is a heavy, brown powder usually processed by sintering, and an important carbide additive material. TaC have high melting temperatures (3880°C) and thermal stability with Fe-based alloys; thus, they are great options for reinforcing tool steels [7]. Our previous study indicated that the transverse rupture strength (TRS) and hardness of the added 10% TaC specimen showed significant improvement [8].

In higher carbon content steels, the martensite finish line temperature is below 0°C, which means that at the end of the heat treatment, a low percentage of austenite is retained at room temperature. The retained austenite as a soft phase in steels could reduce the product life in working conditions [9]. The sub-zero treatment has been acknowledged for many decades as an effective method for increasing wear resistance in tool steels [10]. Vanadis 4 Extra steels contain high amount of carbon and alloying elements (Cr, V, Mo etc.) which remarkably reduce M_f temperature of the steel. By applying sub-zero treatment after quenching to reducing the amount of the austenite is necessary [11]. Das et al. examined the influence of cryogenic

[1] NATIONAL KANGSHAN AGRICULTURAL INDUSTRIAL SENIOR HIGH SCHOOL, DEPARTMENT OF AUTO-MECHANICS KAOHSIUNG 82049, TAIWAN, ROC
[2] NATIONAL TAIPEI UNIVERSITY OF TECHNOLOGY, DEPARTMENT OF MATERIALS AND MINERAL RESOURCES ENGINEERING, TAIPEI 10608, TAIWAN, ROC

* Corresponding author: changsh@ntut.edu.tw

(also called sub-zero) treatment in between quenching and tempering on carbide precipitation of commercial AISI D2 steel. Experimental results showed that the cryogenic treatment of D2 steel reduces the amount of retained austenite and the formation of refined secondary carbides, leads to a more uniform distribution of the carbides than those in conventionally heat treated D2 steel [12]. Koneshlou et al. studied the H13 hot-work tool steel. By applying the sub-zero treatments, the retained austenite was transformed to martensite. The sub-zero treatment also resulted in precipitation of more uniform and very fine carbide particles. The microstructural modification resulted in a significant improvement in the mechanical properties of the H13 tool steel [13]. The aim of this work was to investigate the vacuum sintering and heat treatment processes for V4ES/TaC composites in terms of its microstructure, hardness, TRS and corrosion resistance as well.

2. Experimental procedures

In this study, the gas-atomized Vanadis 4 Extra steel powders are used as a substrate, which showed the spherical particle characteristics. The mean particle size of the Vanadis 4 Extra powders was 48.5±1 μm. The chemical compositions (wt.%) of the Vanadis 4 Extra powders are as follows: 4.7% Cr, 3.7% V, 1.4% C, 3.5% Mo, 0.4% Si, 0.4% Mn and a balance of Fe. In addition, the surface morphology of TaC powders is a polygon, and there were undulating surfaces. The mean particle size of the TaC powders was about 1.78±0.5 μm. Different amounts of TaC powders (5, 10 and 15 wt.%) were mixed and added to Vanadis 4 Extra powders, designated as V4ES/5TAC, V4ES/10TAC and V4ES/15TAC, hereafter. The mixed powders were dry milled by using the WC balls at 250 rpm (set by a planetary ball mill, ITOH Co., LP-1) for 6 h (the weight ratio of ball to powder was 8:1). The morphology under the effect of mechanical alloying by ball milling for 6 h (Fig. 1); the mixed alloy powders produced a significant plastic deformation. TaC is clearly coated on the Vanadis 4 Extra powders, as indicated by the arrows. The surface morphology shows the mechanical interlocking adhesion between the Vanadis 4 Extra powders and TaC powders by ball milling for 6 h. Besides, the mean size of mixed alloy powders reveals a significant decrease (19.0±0.5 μm, which was measured by estimated on SEM pictures).

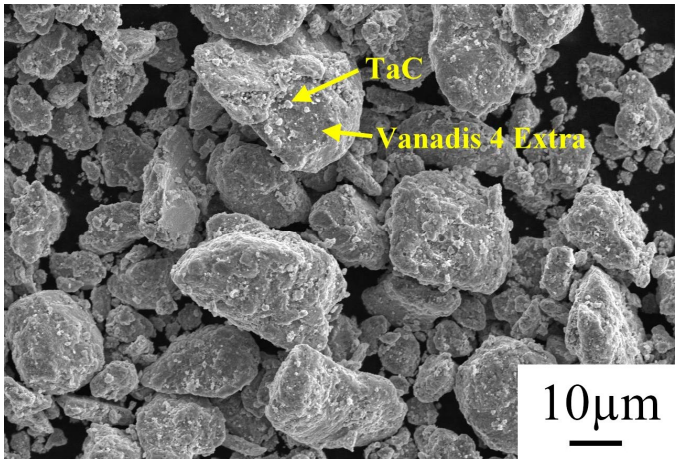

Fig. 1. The SEM images of the surface morphology of V4ES/TaC composite powders after 6 h ball mixing

After milling, the 4 wt.% PVA (polyvinyl alcohol) as a binder was added. The green compact (40×6×6 mm^3) of the powder specimen was produced under a uniaxial pressure at 300 MPa for 300 sec. In this study, the vacuum sintering was conducted at 1260, 1280, 1300, 1320, 1340 and 1360°C for 1 h in a 1.33×10^{-2} Pa, respectively. The cooling rate was 3.3×10^{-1} °C·s^{-1} after sintering. In addition, a series of heat treatments and sub-zero (SZ) heat treatment was performed, by which the optimal parameters of samples were heated to 1020°C and maintained at that temperature for 100 min for quenching, SZ samples with 0.5 MPa of N_2 for quenching media, and then subjected to sub-zero treatment (–150°C for 60 min). Meanwhile, the tempering temperature was held at 540°C for 180 min and repeated three times.

To evaluate the sintered behavior of Vanadis 4 Extra added TaC powders by vacuum sintering and heat treatment, microstructure observations, the apparent porosity, hardness, TRS tests and corrosion tests (Potential Stat Chi 601) were performed. Microstructural observations of the specimens were performed by light microscope (LM, Nikon-Optiphot 66), X-ray diffraction (Bruker/D2 Phaser) and scanning electron microscopy (Hitachi-S4700). The LM specimen was grinded from #120, #600 to #1000 diamond grinding discs, and then polished by 0.3 μm diamond polishing solution. Finally, corrosion the specimen with 10 wt.% Nital solution. Porosity test (apparent porosity) was conducted in accordance to the ASTM C830 standard. Hardness tests were performed by Rockwell hardness tester (HRA, Indentec 8150LK) with a loading of 588.4 N, which followed the ASTM B294 standard. The Hung Ta universal material test machine (HT-9501A) with a maximum load of 245 kN was used for the TRS tests (ASTMB528-12). Meanwhile, R_{bm} was the TRS, which is determined as the fracture stress in the surface zone. F was maximum fracture load, L was 31 mm, k was chamfer correction factor (normally 1.00-1.02), b and h were 5 mm in the equation $R_{bm} = 3FLk/2bh^2$, respectively. The specimen dimensions of the TRS test were 5×5×40 mm^3 and tests at least three pieces.

The corrosion potential analysis uses three electrodes method: the reference electrode is a saturated of silver-silver chloride electrode, auxiliary electrode is a platinum electrode, and the working electrode is connected to the test specimens (ASTM G59-97). The corrosive solvent used 3.5 wt.% NaCl solution and was maintained at room temperature. A scanning speed of 0.01 v·s^{-1}, initial potential of –2.0 V, and the final potential of 2.0 V were controlled. The polarization curve was obtained by Corr-View software to analyze and compare the corrosion potential (E_{corr}) and corrosion current (I_{corr}) of different sintering parameters.

3. Results and discussion

3.1. Effect of sintering temperatures on the microstructure and properties

Volume shrinkage and apparent porosity of examined V4ES/TaC composites depend on TaC content and sintering temperature (Table 1). The volume shrinkage of specimens V4ES/10TAC and V4ES/15TAC were minimal after sintering at 1260°C compared with the Vanadis 4 Extra specimens. It is possible to say that the TaC powders can obstruct diffusion of an atom through the microstructure during the sintering process. As the sintering temperature increased, the volume shrinkage of specimens V4ES/5TAC, V4ES/10TAC and V4ES/15TAC showed a significant increase. Generally, the volume shrinkage of specimens did not obviously increase with the increase in sintering temperatures. This means that the sintered specimens achieved a near full density. Further increasing the sintering temperature will lead to matrix melting, which is not suitable for the P/M sintering. As a result, the more TaC powders that were added, the higher the sintering temperature needed to reach the full density.

As for the apparent porosity level, it displays an inverse proportion to the volume shrinkage of the specimens. The porosities of all specimens decreased as the sintering temperature increased, and the porosity levels of specimens V4ES/5TAC, V4ES/10TAC and V4ES/15TAC were less than 0.4% after sintering at 1300°C, 1320°C and 1340°C for 1 h, respectively. The specimens with more TaC powders added required a higher temperature to provide sufficient energy for a full density of the V4ES/TaC composite. When a solid skeleton develops before full densification during the sintering process, the diffusion stage of densification is often enhanced. In this study, the porosity level of the Vanadis 4 Extra, V4ES/5TAC and V4ES/10TAC specimens obviously decreased to under 0.15%. It is possible to say that the Vanadis 4 Extra, V4ES/5TAC and V4ES/10TAC specimens underwent an appropriate liquid phase diffusion after ideal sintering temperatures. However, the V4ES/15TAC specimen nearly melted after sintering over 1360°C for 1 h, which rendered the specimens unsuitable for subsequent research and testing. Perhaps when fabricating V4ES/TaC composites with a large number of strengthening phases (TaC), other P/M technologies, such as hot isostatic pressing (HIP) can be utilized to improve it.

LM images of the V4ES/TaC composite samples showed similar evolution of their microstructures under different sintering temperatures. Taking the Vanadis 4 Extra specimens sintered at 1260°C and specimens V4ES/5TAC, V4ES/10TAC and V4ES/15TAC sintered at 1300°C for 1 h as examples, the LM images of the Vanadis 4 Extra, V4ES/5TAC, V4ES/10TAC and V4ES/15TAC specimens are shown in Fig. 2. Two type carbides appear in the Vanadis 4 Extra specimen, as shown in Fig. 2a. One is round-shaped carbides which are uniformly distributed within the grains and around the grain boundaries; the other is less plate-like carbides located in the grain boundaries. Previous studies indicated that the round-shaped and plate-like carbides possibly were V-rich MC and Cr-rich M_7C_3 carbides resulting from Vanadis 4 Extra specimens with high vanadium and chromium amounts, respectively. The results will be examined further in subsequent discussions. In addition, there were many TaC particles clustered in the grain boundaries and that increased as the amount of TaC added to the Vanadis 4-Extra increased (the arrow in Figs. 2b-2d). Moreover, a comparison of Figs. 2b, 2c and 2d shows that the amount and size of the residual porosity were significantly increased as the amount of TaC powders added

TABLE 1

Comparison of the volume shrinkage, apparent porosity, grain size, hardness and TRS of V4ES/TaC composite for various sintering temperatures

Temperature (°C)		1260	1280	1300	1320	1340	1360
Volume shrinkage (%)	Vanadis 4 Extra	26.81	26.77	–	–	–	–
	V4ES/5TAC	18.94	27.75	34.85	34.66	–	–
	V4ES/10TAC	8.43	13.42	31.37	34.46	36.68	–
	V4ES/15TAC	2.57	9.28	13.51	35.24	36.83	37.56
Apparent Porosity (%)	Vanadis 4 Extra	0.14	0.13	–	–	–	–
	V4ES/5TAC	7.75	1.61	0.33	0.11	–	–
	V4ES/10TAC	26.22	9.87	1.02	0.18	0.09	–
	V4ES/15TAC	32.53	18.64	5.16	0.73	0.32	0.28
Grain size (μm)	Vanadis 4 Extra	42.9±2.9	77.3±7.3	–	–	–	–
	V4ES/5TAC	10.5±0.4	16.1±0.6	20.3±0.5	36.3±1.3	–	–
	V4ES/10TAC	8.9±0.3	14.2±0.2	18.4±0.5	25.7±1.1	32.3±1.7	–
	V4ES/15TAC	7.1±0.4	12.1±0.3	16.7±0.8	19.3±0.5	22.6±0.8	26.7±1.2
Hardness (HRA)	Vanadis 4 Extra	78.3±0.8	77.5±0.9	–	–	–	–
	V4ES/5TAC	57.5±0.8	71.5±1.4	77.8±0.4	76.9±0.5	–	–
	V4ES/10TAC	48.7±1.2	54.3±0.6	72.6±0.5	79.7±0.4	77.8±0.5	–
	V4ES/15TAC	44.1±1.1	51.9±0.9	57.6±0.7	77.1±0.4	77.3±0.4	78.1±0.6
TRS (MPa)	Vanadis 4 Extra	1522±93.4	1235±28.9	–	–	–	–
	V4ES/5TAC	596±25.2	1363±55.6	2100±30.2	1921±60.1	–	–
	V4ES/10TAC	362±20.2	528±48.2	1723±50.7	2246±79.5	2069±19.9	–
	V4ES/15TAC	203±30.5	266±58.2	724±62.4	1723±47.3	1840±20.6	2029±48.5

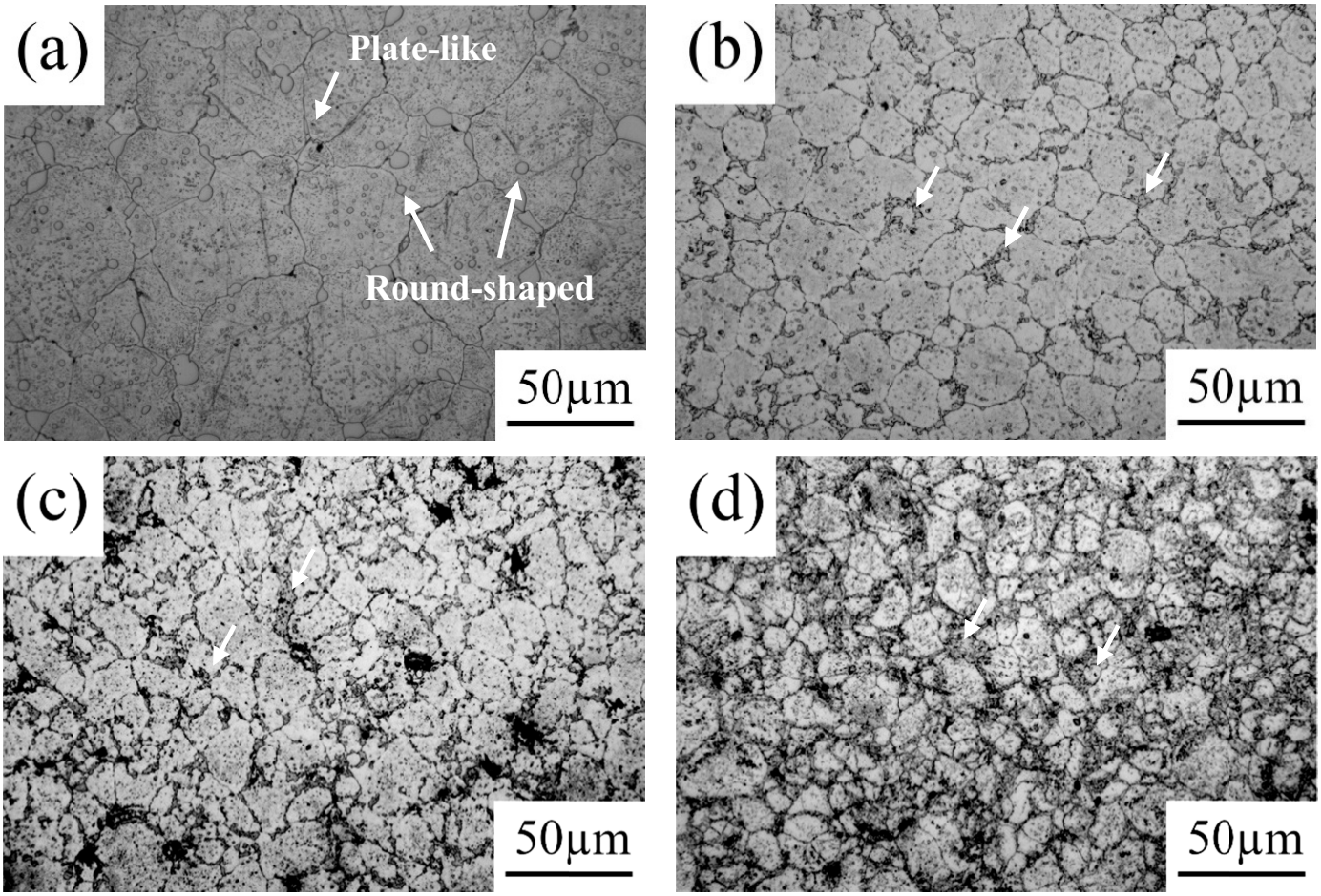

Fig. 2. The LM images of (a) Vanadis 4 Extra sintered at 1260°C, (b) V4ES/5TAC sintered at 1300°C, (c) V4ES/10TAC sintered at 1300°C, and (d) V4ES/15TAC sintered at 1300°C

was increased. The specimens with more TaC powders added required a higher temperature to provide sufficient energy for decreasing the porosity of the V4ES/TaC composite. This can be ascribed to draining off the pores from the high-energy grain boundaries and increasing the density. Fig. 2 also shows that the average grain size decreased as the amount of added TaC increased. In this study, the average grain size was measured by linear intercept method. The average grain size of V4ES/5TAC, V4ES/10TAC and V4ES/15TAC showed a significant decrease (20.3 → 18.4 → 16.7 μm). Apparently, the TaC located in the grain boundaries played an important role in inhibiting grain growth during the sintering process.

The microstructural observation of Vanadis 4 Extra and V4ES/10TAC specimens after sintering at 1260°C and 1320°C were analyzed by SEM and EDS, respectively (Fig. 3). As Fig. 3a shows, carbides that were less plate-like (grey color) appeared in the grain boundaries, and the round-shaped carbides (black color) were distributed around the grain boundaries and within the grains. The EDS analysis results revealed that the plate-like carbides (Location 1) in the grain boundaries and the round-shaped carbides (Location 2) within the matrixes were M_7C_3 carbides and MC carbides, respectively. Moreover, all V4ES/TaC composite had a similar morphology and compositions of carbide. Taking the specimen V4ES/10TAC sintered at 1320°C for 1 h as an example, as seen in Fig. 3b, a few round-shaped carbides uniformly surrounding the grain boundaries can be observed. The EDS analysis results revealed that the round-shaped carbides surrounding the grain boundaries (Location 3) were TaC and a high content of V-rich VC carbides; the compositions are listed in Fig. 3c. Since the clustered TaC and VC carbides in the grain boundaries appeared to replace the plate-like carbides (Vanadis 4 Extra), it is reasonable to suggest that the TaC served as the nucleation sites of the VC carbides, which resulted in the generation of VC carbides in the grain boundaries. Besides, the EDS analysis results revealed that the particle-like carbides within the grains (Location 4) were V-rich VC carbides; the compositions are listed in Fig. 3c. When the sintering temperature was raised, the particle-like VC carbides within the grains possessed enough energy to diffuse to the grain boundaries resulting in a decrease in the volume fraction of the carbides.

Mechanical properties of the Vanadis 4 Extra, V4ES/5TAC, V4ES/10TAC and V4ES/15TAC specimens after various sintering temperatures were performed by the hardness and TRS tests (Fig. 4). As Fig. 4a shows, the hardness of specimens V4ES/5TAC and V4ES/10TAC first increased and then decreased. Besides, the hardness of the V4ES/15TAC specimens first increased and then remained flat. The V4ES/10TAC specimens possessed the highest hardness (79.7 HRA) after sintering

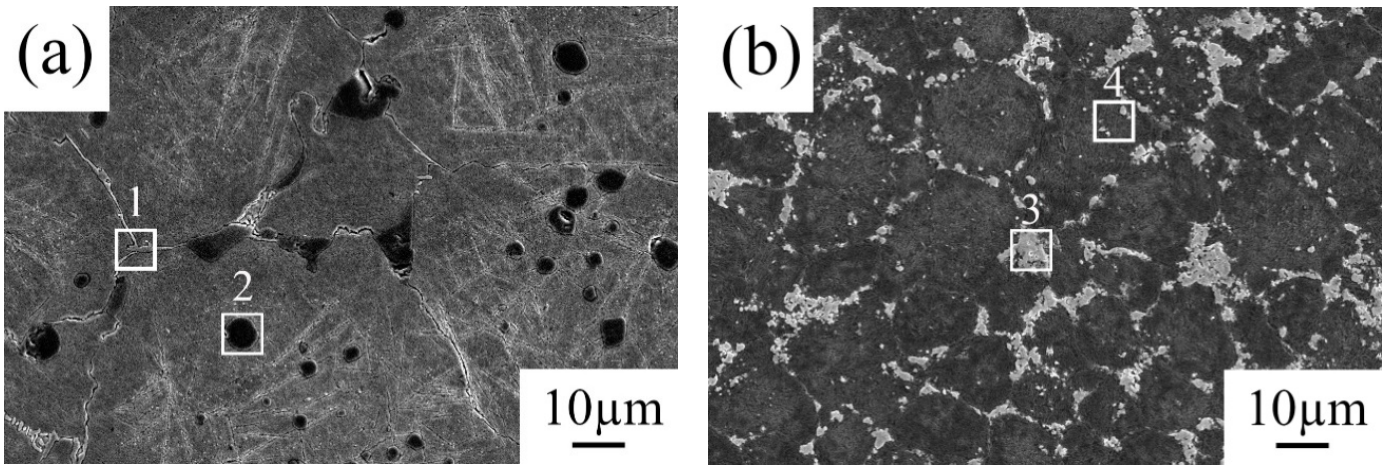

	Location 1		Location 2		Location 3		Location 4	
Element	**Weight%**	**Atomic%**	**Weight%**	**Atomic%**	**Weight%**	**Atomic%**	**Weight%**	**Atomic%**
C	18.86	55.91	21.23	55.65	16.55	67.54	15.75	57.41
V	6.41	4.45	58.11	35.92	10.69	10.29	22.46	19.30
Cr	15.01	9.95	4.14	2.51	–	–	2.20	1.85
Fe	28.71	18.21	2.15	1.21	2.49	2.18	8.24	6.46
Mo	30.90	11.40	14.37	4.72	3.95	2.02	11.86	5.41
Ta	–	–	–	–	66.33	17.97	39.51	9.56

Fig. 3. The SEM images and EDS analysis of (a) Vanadis 4 Extra sintered at 1260°C, (b) V4ES/10TAC sintered at 1320°C

at 1320°C. Our previous study indicated that the hardness value of 440C steel composites is in reverse proportion to the porosity level [14]. Table 1 also listed that the hardness and TRS of all specimens was relative to the porosity level after sintering at different sintering temperatures (the scatter intervals are simply standard deviation). The results show that the sintering temperatures of 1260 and 1280°C for V4ES/TaC composite materials was not high enough. Besides, the hardness values of the V4ES/10TAC specimens (79.7 HRA) were higher than those of Vanadis 4-Extra specimens (78.3 HRA) with optimal sintering temperatures. On the other hand, the hardness values of the Vanadis 4 Extra, V4ES/5TAC and V4ES/10TAC specimens tended to decrease slightly resulting from the grain coarsening after sintering at 1280, 1320 and 1340°C, respectively. As for the V4ES/15TAC specimens, although the sintering temperature increased to 1360°C, the porosity level was still 0.28% resulting in a lower hardness value.

The typical TRS curves of specimens V4ES/5TAC and V4ES/10TAC first increased and then, decreased while the V4ES/15TAC specimens kept increasing as the sintering temperature increased (Fig. 4b). The variations in TRS values are similar to those of the hardness values. The V4ES/5TAC specimens possessed better TRS after sintering at 1300°C compared with the Vanadis 4-Extra specimens, while the V4ES/10TAC specimens have the highest TRS (2246 MPa) after sintering at 1320°C. Our previous study indicated that the precipitated refined carbides

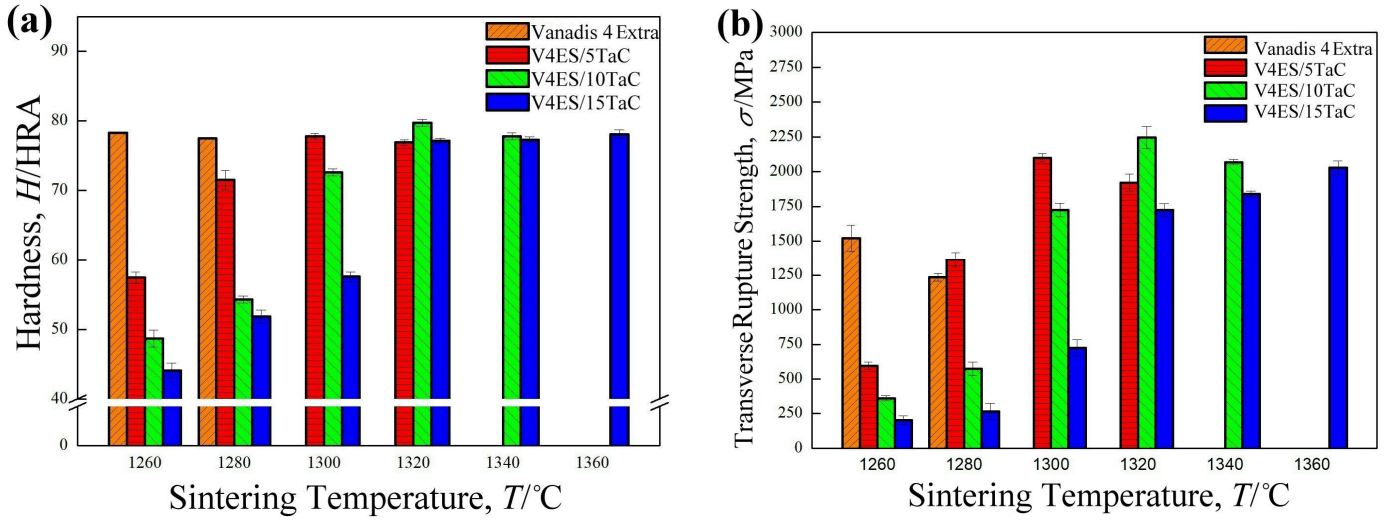

Fig. 4. Comparison of the hardness and TRS of various wt.% TaC added Vanadis 4 Extra by the different sintering temperatures

and porosity levels of Vanadis 4 composites are important factors that directly affect the TRS [9,15]. If the sintered specimen was not fully densified, the materials possessed numerous small pores. When the specimen was subjected to extra stress during the TRS tests, cracks grew along the internal pores, resulting in rapid fracturing. In addition, Fig. 3b shows that the clustered TaC carbides in the grain boundaries and the particle-like carbides within the grains show uniform distribution. The carbides are able to resist the movement of dislocation, which is advantageous to TRS. From the above-mentioned discussion, the V4ES/10TAC specimens must reach 1320°C to gain a fully densified microstructure (Table 1) resulting in the highest TRS value. Moreover, the TRS values of V4ES/10TAC specimens decreased as the sintering temperature increased to 1340°C. Although the porosity of the V4ES/10TAC specimens decreased less than 0.09%, the higher sintering temperature (1340°C) caused a grain-coarsening phenomenon which seemed to significantly affect the TRS values. However, the grain coarsening phenomenon is not the only factor that affects the TRS value. When the sintering temperature is increased to 1340°C, the particle-like VC carbides within the grains diffuse to the grain boundaries resulting in a decrease in the volume fraction of the carbides which also affects the TRS. Thus, the particle-like carbides VC uniformly dispersed within the grains, and the clustered TaC and VC carbides distributed around the grain boundaries after sintering at 1320°C. Those results were advantageous to the TRS.

Further examination of the fracture feature of Vanadis 4 Extra specimens sintered at 1260°C and V4ES/10TAC sintered at 1320°C (Fig. 5), many dimples and some transgranular cleavage fractures could be observed (Fig. 5a). The ductile behavior is the main fracture characteristic, which is ascribed to a full density of Vanadis 4 Extra specimens. However, when the sintering temperature increased to 1280°C, the Vanadis 4 Extra specimens caused a grain-coarsening phenomenon which led to a more brittle cleavage feature. In addition, the sintered V4ES/10TAC specimen had many pores in the matrix until the temperature reached 1300°C. When the sintering temperature was raised to 1320°C, many dimples and some small cleavages could be observed, as shown in Fig. 5b. The presence of a greater number of dislocations was generated by the plastic extension when the fracture was under continually increasing loads. The carbides in the matrix resisted the movement of dislocation, and then, the strength improved [16]. Meanwhile, the carbides broke up into smaller particles during deformation resulting from the ductile behavior. Increasing the sintering temperature (1340°C) leads to a grain-coarsening phenomenon. Although the fracture feature is similar to that shown in Fig. 5b, grain coarsening is easier to generate on a flat fracture feature which is disadvantageous to the TRS.

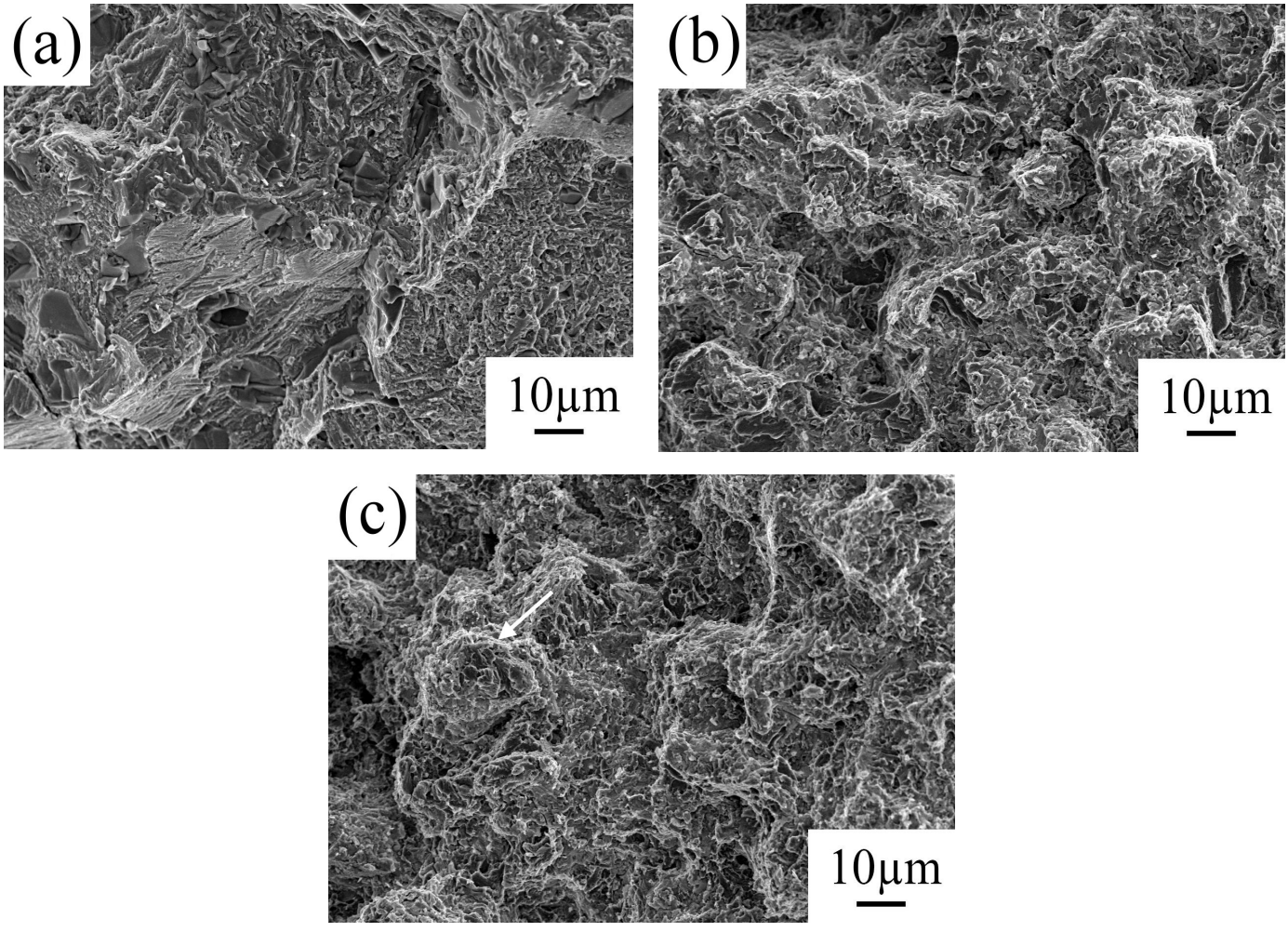

Fig. 5. The fracture surfaces of (a) Vanadis 4 Extra sintered at 1260°C, (b) V4ES/10TAC sintered at 1320°C, (c) SZ-V4ES/10TAC specimen

TABLE 2

Comparison of the corrosion results of V4ES/TaC composite after sintering at 1320°C and sub-zero heat treatments after 3.5 wt.% NaCl corrosion tests

	Vanadis 4 Extra	V4ES/5TAC	V4ES/10TAC	V4ES/15TAC	HT-V4ES/10TAC	SZ-V4ES/10TAC	SZ-Vanadis 4 Extra
I_o ($\times 10^{-4}$ A·cm^{-2})	3.95	4.48	4.88	5.37	1.59	1.23	0.62
E_o (Volts)	–0.80	–0.81	–0.83	–0.82	–0.84	–0.84	–0.86
R_P (Ω·cm^2)	304.33	292.77	299.82	275.12	526.23	658.99	1006.52

In addition, comparison of the corrosion properties for sintered specimens V4ES/5TAC, V4ES/10TAC and V4ES/15TAC sintered at 1320°C as well as 1260°C-sintered Vanadis 4 Extra after the 3.5 wt.% NaCl corrosion test (Table 2). In general, in an electrochemical reaction, higher polarization resistance usually means better corrosion resistance. The apparent porosity should be the main factor affecting corrosion resistance. Besides, the carbides precipitated are another factor that affects the corrosion resistance. The higher the amount of TaC added to Vanadis 4 Extra, the more carbides that are precipitated in the grain boundaries. The grain boundaries act as a site where not only orientation but also chemistry undergoes an abrupt transition. Also, segregation of a phase active in certain atmospheres also raises the energy at the grain boundaries. Excess carbides precipitated in the grain boundaries easily caused electrochemical non-uniformity resulting in intergranular corrosion [17]. This is why Vanadis 4 Extra specimens possess the highest corrosion resistance while V4ES/10TAC specimens possess a higher corrosive resistance.

3.2. Effect of heat treatments on the microstructure and properties

By using the XRD patterns to analyze the crystal orientation of the V4ES/10TAC specimens after different heat treatments (Fig. 6a). The V4ES/10TAC and SZ-V4ES/10TAC have similar diffraction peaks at the TaC phase and possess a typical martensite structure (α-Fe). However, austenite peaks were generated on the specimens (HT-V4ES/10TAC) after the sintering and heat treatment processes. It is suitable to say that the austenite phase did not completely transform to the martensite phase after the quenching process, which was disadvantageous to the mechanical properties. It was found that by applying sub-zero treatments, the retained austenite was significantly transformed to martensite.

A detailed analysis of internal structure of the V4ES/10TAC specimen after different heat treatments by the SEM images of (Fig. 7a). The size of grey carbides (Location 1) around the grain boundaries show a slight decrease after heat treatment compared with the V4ES/10TAC specimens (Fig. 3b). Meanwhile, a few refined carbides were generated within the grains. A reasonable explanation for this effect is that parts of VC carbides dissolved into the matrix, while the refined particle-like carbides (Location 2) within the grains re-precipitated. The EDS analysis results reveal that the grey carbides (Location 1) were V-rich TaC carbides, and the refined particle-like carbides (Location 2) were V rich VC carbides. It is reasonable to say that the VC carbides re-precipitated within the grains did not have enough time to diffuse to the grain boundaries during the quenching and tempering process. In addition, the microstructure of SZ-V4ES/10TAC was a little different than that of the

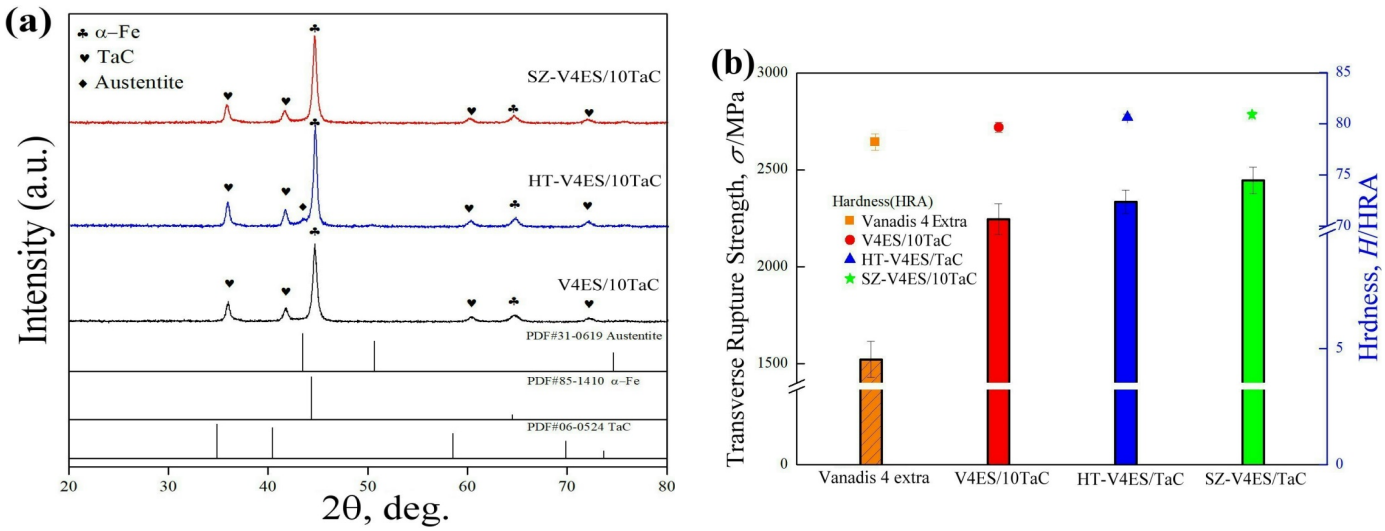

Fig. 6. XRD analysis, hardness and TRS of the optimal V4ES/TaC composite specimens (V4ES/10TAC) after different heat treatments (a) XRD analysis, (b) hardness and TRS

HT-V4ES/10TAC specimens. The VC carbides re-precipitated within the grains became more uniform, and the microstructure, except the retained austenite, was transformed to martensite, as shown in Fig. 7b. Moreover, the clustered carbides (TaC) formed in the grain boundaries during the sintering process, and the heat treatments could not change the distribution of the TaC particles, they could only control the shape and distribution of the VC carbides. Thus, TaC powders added to Vanadis 4 Extra as a strengthening phase made them pile up and cluster in the grain boundaries (Fig. 7). The results confirmed that the VC carbides decomposed and re-precipitated as refined VC carbides within the grains after the heat treatment.

In this study, the hardness of the V4ES/10TAC sample was about 79.7 HRA whereas the hardness values of the HT-V4ES/10TAC and SZ-V4ES/10TAC samples were about 80.6 HRA and 80.9 HRA, respectively. It is possible to say that the high hardness of the HT-V4ES/10TAC sample is due to martensite morphology, alloying elements in the martensite and retained austenite. In addition, sub-zero heat treatment could have encouraged carbide formation during tempering, leading to increased hardness [9]. A previous study indicated that in sub-zero and heat treatment, the variations in hardness were possibly dominated by the tempering process, which released the internal stress from the tempering treatment [11]. As a result, a slight increase in hardness could be ascribed to the re-precipitated refined carbides' uniform distribution in the matrix.

As for the TRS, the HT-V4ES/10TAC and SZ-V4ES/10TAC specimens revealed a significant increase, as shown in Fig. 6b. The TRS value is increased from 2246 MPa to 2335 MPa (HT-V4ES/10TAC) and 2445 MPa (SZ-V4ES/10TAC). Generally speaking, a suitable amount of carbides uniformly re-precipitated within the grains resulted in increased TRS. Moreover, an inverse relationship exists between the strength of the martensite formed in the quenching process and the amount of residual austenite; the martensite's strength increases as the amount of retained austenite decreases [18]. However, J.D. Escobar et al. stated that the existence of austenite in hard steels is not always bad [19-21]. In other words, the appropriate content of retained austenite can increase the toughness of alloy steels. In this study, the sub-zero heat treatment process improved the redistribution of the refined VC carbides in the matrix and the transformation of the retained austenite to martensite for the SZ-V4ES/10TAC samples. Thus, the TRS of the SZ-V4ES/10TAC specimens revealed a significant increase resulting from the dispersion strengthening and precipitation hardening effects. The fracture surface of such a ductile fracture showed a dimpled feature when observed on SEM images, as shown in Fig. 5c. The fracture surface observation also found many small voids, which would have been from the breaking away of refined carbides which left the voids. Besides, the fracture surface appears as spider web-like dimpled ruptures.

Furthermore, to compare the corrosion properties for HT-V4ES/10TAC and SZ-V4ES/10TAC specimens after 3.5 wt.% NaCl corrosion tests (Table 2). The corrosion resistance of the V4ES/10TAC specimens had a significant variation after the different heat treatments. The polarization resistance (R_p = 658.99 Ω·cm^2) of the SZ-V4ES/10TAC specimens shows a significant improvement that is better than the Vanadis 4 Extra specimens (R_p = 304.33 Ω·cm^2). In addition, the current value represents the diversification of the equilibrium constants in the oxidation reaction. If the current value is higher, it leads to an increase in the equilibrium constant and a fast oxidation.

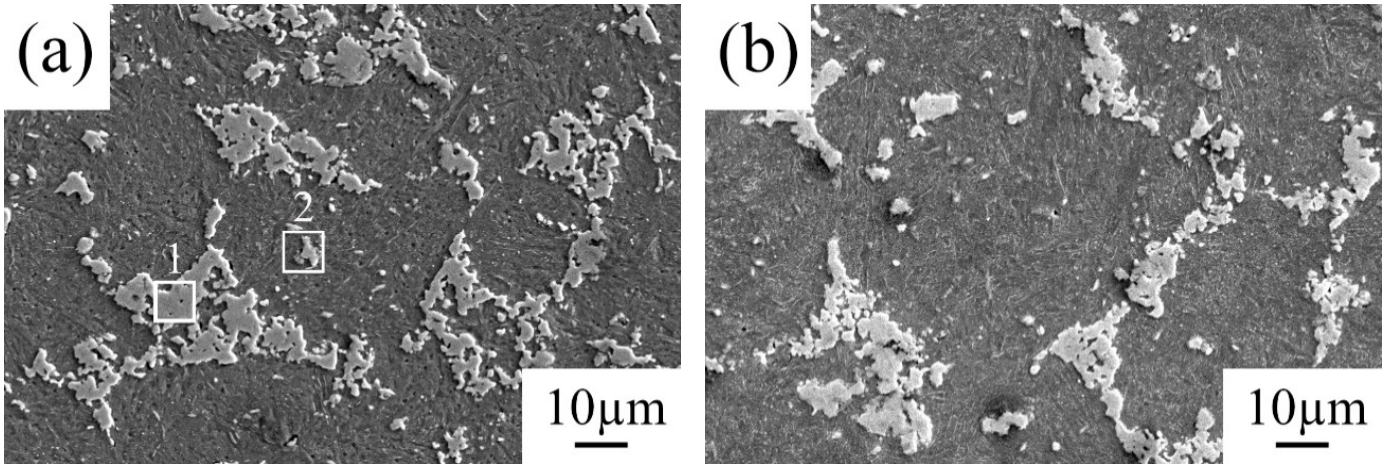

	Location 1		Location 2	
Element	**Weight%**	**Atomic%**	**Weight%**	**Atomic%**
C	10.62	54.93	7.50	39.56
V	11.68	14.25	17.05	21.20
Fe	3.08	3.43	13.47	15.28
Mo	5.79	3.75	7.26	4.79
Ta	68.83	23.64	54.72	19.16

Fig. 7. The SEM images and EDS analysis of (a) HT-V4ES/10TAC, (b) SZ-V4ES/10TAC

A lower corrosion current (I_{corr} = 1.23×10^{-4} A·cm^{-2}) appeared in the SZ-V4ES/10TAC specimens. It is possible to say that parts of the VC carbides dissolving and refined VC carbides re-precipitating within the grains after the sub-zero heat treatment resulted in a significant improvement in corrosion resistance. However, the corrosion resistance of the SZ-V4ES/10TAC specimens is still not better than that of Vanadis 4 Extra specimens. It is reasonable to infer that the porosity between TaC particles cannot be completely eliminated after sub-zero heat treatment; moreover, the TaC carbides did not dissolve into the matrix but piled up in the grain boundaries. Both of them are disadvantageous to corrosion resistance. Although the sub-zero heat treatment did not improve the corrosion resistance of the V4ES/TaC composites, it is possible to suggest that the SZ-V4ES/10TAC specimens were sintered at 1320°C for 1 h, followed by a sub-zero heat treatment, which possessed optimal mechanical properties and suitable anti-corrosion ability in the 3.5 wt.% NaCl solution.

4. Conclusions

According to the experimental results discussed in the previous sections, the following conclusions can be drawn:

(1) The addition of 10 wt.% TaC to Vanadis 4 Extra steel powder enables to obtain in vacuum sintering at 1320°C for 1 h a composite characterized by good mechanical properties – TRS and hardness reached 2246 MPa and 79.7 HRA, respectively – and relative low apparent porosity – 0.18%.

(2) For the V4ES/10TAC specimens, the clustered TaC particles were located on the grain boundaries. Moreover, the TaC served as the nucleation sites for the VC carbides which were precipitated in the grain boundaries. Meanwhile, the particle-like VC carbides uniformly appeared within the grains after optimal sintering temperatures. When the optimally sintered specimens underwent a series of sub-zero heat treatments, parts of the VC carbides decomposed and re-precipitated as refined VC carbides within the grains, which resulted in dispersion strengthening and precipitation hardening, thereby increasing the hardness and TRS of the V4ES/TaC composites.

(3) Sub-zero heat treatment effectively improved the size of the VC carbides and mechanical properties of the V4ES/TaC composites. Besides, the corrosive resistance displayed a slight increase but still was not better than that of the Vanadis 4 Extra sample after sub-zero treatment. The optimal TRS (2246 MPa) and hardness (80.9 HRA), as well as a suitable corrosion resistance (R_p = 658.99 Ω·cm^2) were obtained for Vanadis 4 Extra by adding 10% TaC after sintering at 1320°C for 1 h, as well as undergoing a series of sub-zero heat treatments.

Acknowledgments

This research is supported by the VOESTALPINE HIGH PERFORMANCE METALS PACIFIC PTE. LTD and ASSAB STEELS TAIWAN CO., LTD. The authors would like to express their appreciation for Dr. Harvard Chen, Michael Liao and Mr. Meng-Yu Liu.

REFERENCE

[1] M. Rahimian, N. Parvin, N. Ehsani, Materials and Design **32**, 1031-1038 (2011).
[2] D.L. Zhang, Progress in Materials Science **49**, 537-560 (2004).
[3] K.T. Huang, S.H. Chang, P.T. Yeh, ISIJ International **57**, 1252-1260 (2017).
[4] M. Rahimiana, N. Ehsani, N. Parvin, H.R. Baharvandi, Journal of Materials Processing Technology **209**, 5387-5393 (2009).
[5] J. Weidow, H.O. Andrén, International Journal of Refractory Metals and Hard Materials **29**, 38-43 (2011).
[6] T.B. Trung, H. Zuhailawati, Z.A. Ahmad, K.N. Ishihara, Journal of Alloys and Compounds **552**, 20-25 (2013).
[7] M. Mahmoodan, H. Aliakbarzadeh, R. Gholamipour, Transactions of Nonferrous Metals Society of China **21**, 1080-1084 (2011).
[8] S.H. Chang, T.P. Tang, K.T. Huang, F.C. Tai, Powder Metallurgy **54**, 507-512 (2011).
[9] F.K. Arslan, I. Altinsoy, A. Hatman, M. Ipek, S. Zeytin, C. Bindal, Vacuum **86**, 370-373 (2011).
[10] D.M. Lal, S. Renganarayanan, A. Kalanidhi, Cryogenics **41**, 149-155 (2001).
[11] H.X. Chi, D.S. Ma, Q.L. Yong, L.Z. Wu, Z.P. Zhang, Y.W. Wang, Journal of Iron and Steel Research International **17**, 43-46 (2010).
[12] D. Das, K. Dutta, V. Toppo, K.K. Ray, Materials and Manufacturing Processes **22**, 474-480 (2007).
[13] M. Koneshlou, K.M. Asl, F. Khomamizadeh, Cryogenics **51**, 55-61 (2011).
[14] K.T. Huang, S.H. Chang, C.K. Wang, J.K. Chen, Materials Transactions **56**, 1585-1590 (2015).
[15] S.H. Chang, P.T. Yeh, K.T. Huang, Vacuum **142**, 123-130 (2017).
[16] S.H. Chang, P.Y. Chang, Materials Science and Engineering: A **606**, 150-156 (2014).
[17] C.S. Tedmon Jr, D.A. Vermilyea, J.H. Rosolowski, Journal of the Electrochemical Society **118**, 192-202 (1971).
[18] D. Scott, J. Blackwell, Wear **18**, 19-28 (1971).
[19] J.D. Escobar, G.A. Faria, E.L. Maia, J.P. Oliveira, T. Boll, S. Seils, P.R. Mei, A.J. Ramirez, Acta Materialia **174**, 246-259 (2019).
[20] J.D. Escobar, J.P. Oliveira, C.A.F. Salvador, G.A. Faria, J.D. Poplawsky, J. Rodriguez, P.R.Mei, S.S. Babu, A.J. Ramirez, Materials and Design **156**, 609-621 (2018).
[21] J.D. Escobar, J.D. Poplawsky, G.A. Faria, J. Rodriguez, J.P. Oliveira, C.A.F. Salvador, P.R.Mei, S.S. Babu, A.J. Ramirez, Materials and Design **140**, 95-105 (2018).